Electronic Supplementary Material (ESI) for ChemComm.

Supporting Information

Investigation of $K_3V_2(PO_4)_3$/C nanocomposite as high-potential cathode materials for potassium-ion batteries

Jin Han,[a,b] Guan-Nan Li,[a] Feng Liu,[a,b] Minqiang Wang,[a,b] Yan Zhang,[a,b] Linyu Hu,[a,b] Chunlong Dai,[a,b] and Maowen Xu[a,b*]

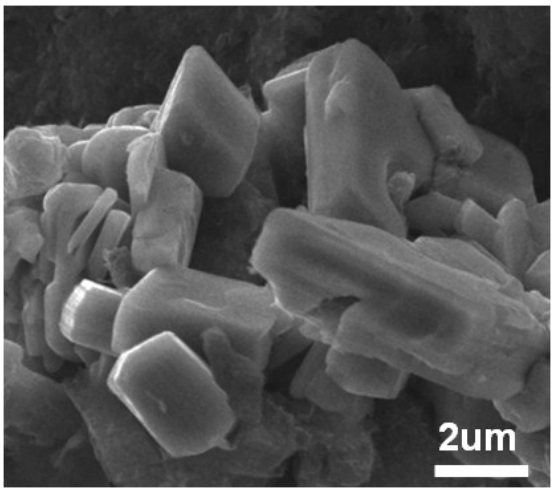

Fig. S1. SEM images of the bulk $K_3V_2(PO_4)_3$.

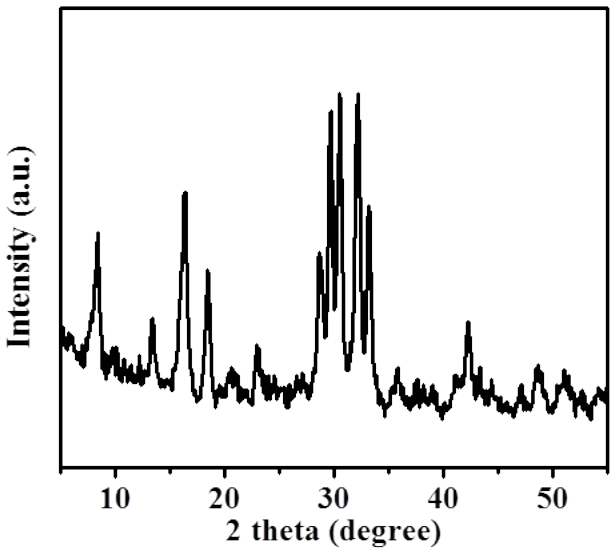

Fig. S2. XRD of the bulk $K_3V_2(PO_4)_3$.

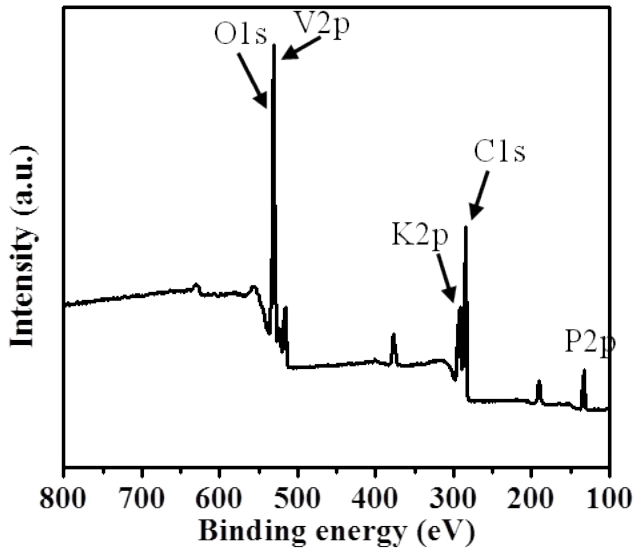

Fig. S3. XPS of $K_3V_2(PO_4)_3$/C before cycle.

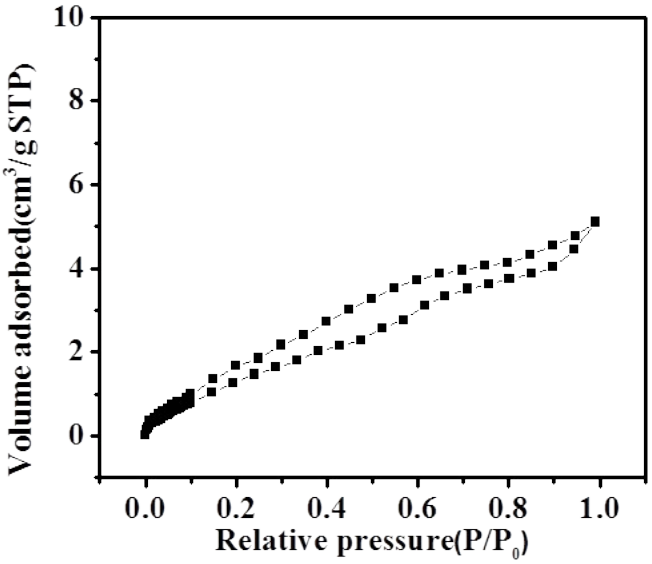

Fig. S4. N_2 adsorption-desorption isotherms of the bulk $K_3V_2(PO_4)_3$

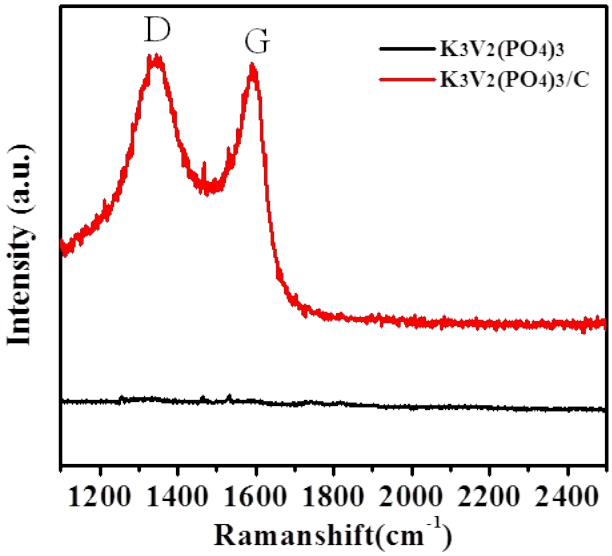

Fig. S5. Raman spectra of the bulk $K_3V_2(PO_4)_3$ and the $K_3V_2(PO_4)_3$/C, respectively;

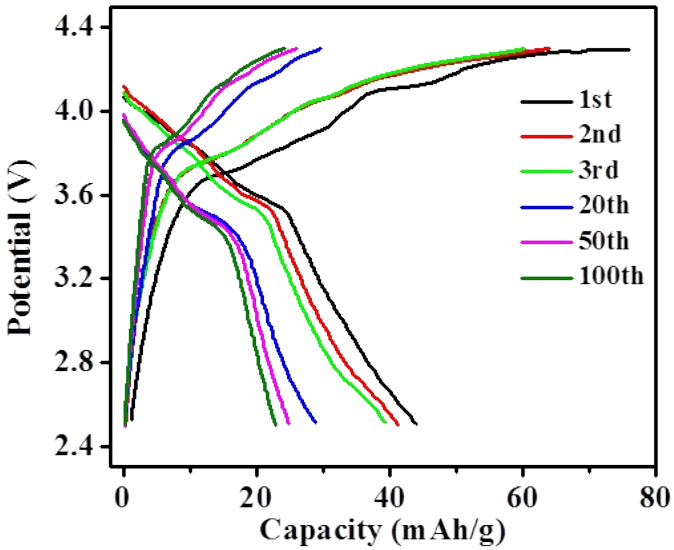

Fig. S6. The different discharge/charge curves of the bulk $K_3V_2(PO_4)_3$ at the current density of 20 mA g^{-1} in the voltage range of 2.5 ~ 4.3 V versus K^+/K;

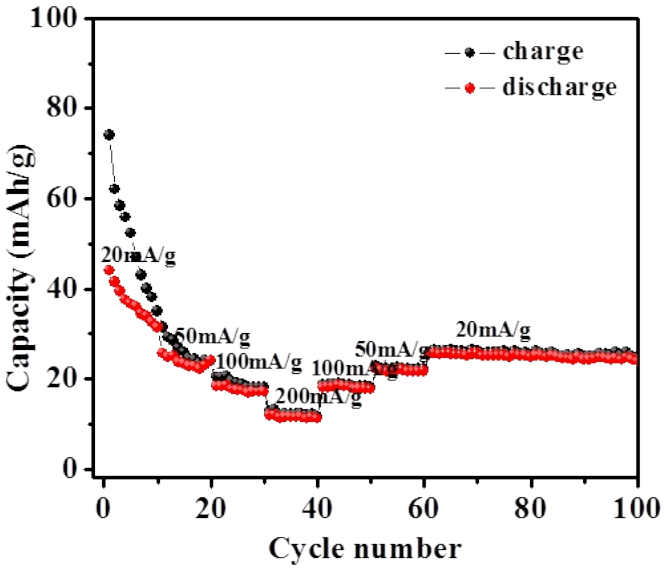

Fig. S7. Rate capability of the bulk $K_3V_2(PO_4)_3$ at the different current density;

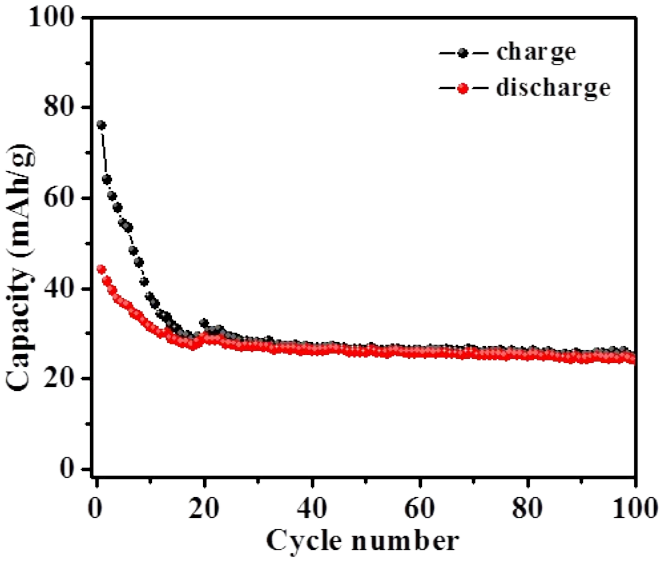

Fig. S8. Cycling performance of the bulk $K_3V_2(PO_4)_3$ at the current density of 20mA g^{-1}.

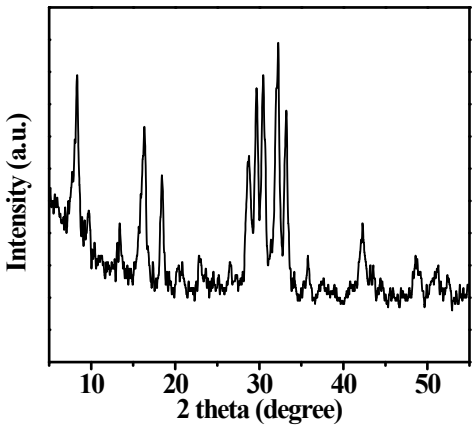

Fig. S9. XRD of the bulk $K_3V_2(PO_4)_3$ electrode after 20 cycles.

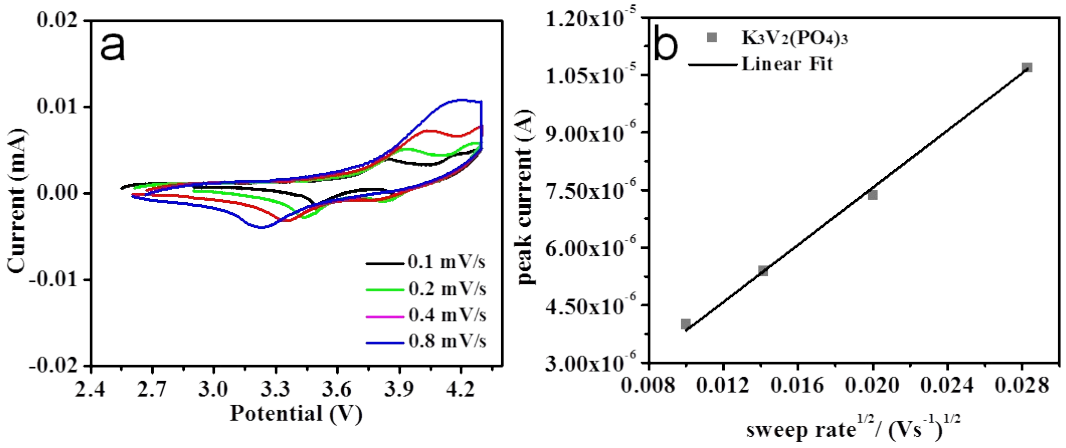

Fig. S10. CV curves of the bulk $K_3V_2(PO_4)_3$ at various scan rates from 0.1 to 0.8 mV s^{-1}, respectively; (d) The absolute value of oxidized peak currents *vs.* the square root of the scan rate plots for the $K_3V_2(PO_4)_3$.

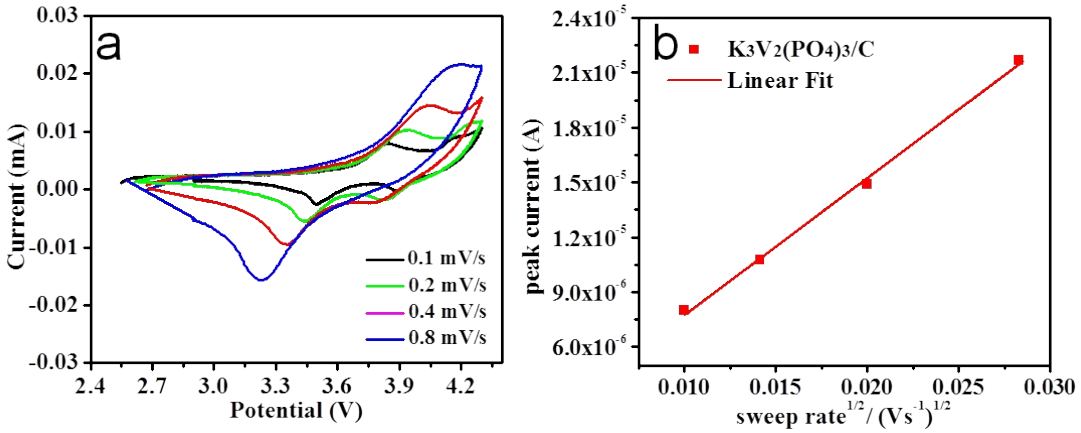

Fig. S11. (a) CV curves of the $K_3V_2(PO_4)_3$/C at various scan rates from 0.1 to 0.8 mV s^{-1}, respectively; (b) The absolute value of oxidized peak currents *vs.* the square root of the scan rate plots for the $K_3V_2(PO_4)_3$/C;

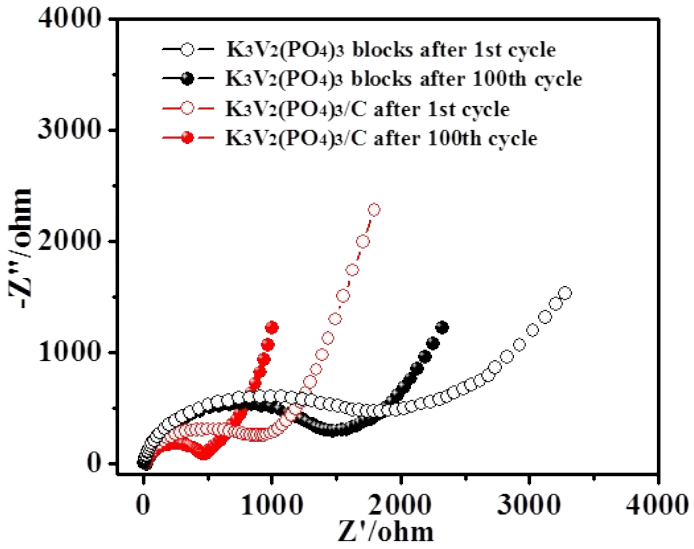

Fig. S12. EIS of the electrodes of the bulk $K_3V_2(PO_4)_3$ and the $K_3V_2(PO_4)_3$/C after 1 cycles and after 100 cycle, respectively.